Journal of Population Therapeutics & Clinical Pharmacology

RESEARCH ARTICLE
DOI: 10.53555/2bky4n93

EXPLORING HIV-1 TAT PENETRABILITY IN TUMOR SPHEROIDS THROUGH CONFOCAL MICROSCOPY: A CELL LINES BASED STUDY

Aziz Ur Rahman[1], Abdullah[2], Muhammad Masoom Akhtar[3], Sheikh Abdur Rashid[4*], Pervaiz Akhtar Shah[5], Mobina Manzoor[6], Jahangir Khan[7], Saima Mahmood[8], Rukhsana Ghaffar[9], Saeed Ahmad[10], Tariq Javed[11*]

[1,2,7,9]Department of Pharmacy, University of Malakand, Pakistan; [1]Email: azizuom123@gmail.com; [2]Email: uom_abdullah@yahoo.com; [7]Email: jahangirkhan222@gmail.com; [9]Email: dr.rghaffar@gmail.com
[1]Manchester Pharmacy School, The University of Manchester, UK; [1]Email: azizuom123@gmail.com
[3]Department of Pharmacology, Faculty of Pharmacy, Hamdard University, Islamabad Campus, Pakistan 44000; [3]Email: m.masoom@hamdard.edu.pk
[4*,8]Gomal Centre of Pharmaceutical Sciences, Faculty of Pharmacy, Gomal University, Dera Ismail Khan, 29050, Pakistan; [4*]Email: sheikhabdurrashid11@gmail.com; [8]Email: saimamahmoodgu@gmail.com
[5]Punjab University College of Pharmacy, University of the Punjab, Lahore, Pakistan, Allama Iqbal Campus, Lahore 54000; [5]Email: pervaiz.pharmacy@pu.edu.pk
[6]Lahore College for Women University; [6]Email: mobina_star@hotmail.com
[10]Department of Zoology, University of Malakand, Pakistan; [10]Email: abutalha_uom@yahoo.com
[11*]Margalla College of Pharmacy, Margalla Institute of Health Sciences, Rawalpindi 46000 Pakistan; [11*]Email: tariqbaghi@gmail.com

***Corresponding Authors:** Sheikh Abdur Rashid & Tariq Javed
*Email: sheikhabdurrashid11@gmail.com, tariqbaghi@gmail.com

ABSTRACT

Deficient vascular supply, intracellular matrix and hypoxia in solid tumor offer hindrance to penetration of drugs into desired site of action. HIV-1 TAT (Human Immunodiffiency Virus type-1 Transactivation of Transcription) peptide reported to penetrate in all stages of cell cycle, and therefore, could be exploited as potential drug carrier to overcome the penetratibility hindrance into resistant tumor tissues. Multicellular tumor spheroids (MCTS) is an *in-vitro* tumor model to measure the penetration of TAT to mimic with *in-vivo* tumors. The current study involves investigation of the penetration rate, penetration depth, peptide accummulation, and extent of TAT penetration in MCTS at 4°C and 37°C for an incubation time of 1.5 hours. Observations were taken at 10 minutes interval, from spheroid surface to the deeper layers through 3µm continous laser sectioning. TAT-labelled fluorescence accumulated approximately at the same rate at each observed depth of MCTS. Moreover, higher accummulation in three-day old spheroids was observed, that could be due to loose packed cells, more ratio of extracellular volume, and more number of live proliferating cells as compared to five-day old spheroids. Detection of penetration and fluorescence

accummulation decreased as spheroids get older, that dependent on multifunctional characteristic along age/duration of cell culture.

Keywords: Peptide drug carrier, Multicellular tumor spheroids, *In-vitro* tumor model, Quantitive measurement, Confocal microscopy, Trans-activation.

1. Introduction

Multicellular Tumor Spheroids (MCTS) model is an intermediate between 2-D cell culture and the *in-vivo* tumors. The 3-D structure of MCTS mimics nonvascularized microtumors (1). MCTS are appropriate models for in-vitro drug delivery testing.Spheroids model possessing critical physiologic characteristics present *in-vivo*, such as complex tissue multicellular architecture, penetration barriers, as well as extracellular matrix (ECM) deposition. Multicellular spheroids model are considered as a useful *in-vitro* tool for drug screening and for estimation of drug delivery to pathological tissues and organs (2). To bridge the gap between laboratory results, preclinical model animals and clinical outcomes necessitate the comprehensive drug screening by using powerful *in-vitro* MCTS models (1). Penetration into the MCTS represents a balance between diffusion in the extracellular space *versus* binding to cell surface and hence subsequent internalization into the cell. It has been reported that the penetration of molecules into the cell vary with temperature (3). The penetration of molecules also depend upon the age of spheroids due to distinct regions in more mature / larger spheroids (4,{Ur Rahman, 2020 #640}). The pathway and mechanism of Cell Penetrating Peptides (CPPs) and cargo internalization depend on the nature of the peptide/cargo (6), the size of the cargo, the cell line in which internalization is under examination (7-10) and the receptor involved (11). The process of penetration may take place by more than one mechanism which depends on the nature of CPP and the microenvironment (11-14). The abnormal architecture plus composition of solid tumours, especially in poorly perfused (avascular) regions, hinder the penetration and distribution of antitumor drugs and thus generate treatment resistance, because intercellular diffusion as well as intracelular retention of anticancer drug is mandatory for therapeutic response. When tumor vasculature is leaked-out, chemotherapeutic agents will penetrate deeply in the avascular regions into the tumor cells (15), and therapeutic response will be achieved.

CPPs possess wide range of therapeutic and biomedical applications including capability of overcoming the lipophilic barriers of cell membrane to ensure the penetrability of cargoes such as antibodies, DNA, and nanoparticular drug carriers into cells and tumor tissues (16,17). In 1988, it was investigated by Green and Loewenstein that HIV-1 TAT (human immunodeficiency virus type-1, trans-activator of transcription) peptide and its distinct fragments penetrate into cell membrane and get localize in cytoplasm as well as in nucleus (18). Commetantly, such a study was also reported in the same year (19). Interestingly, TAT-mediated protein delivery into the cells was reported as a result of which TAT-mediated drug delivery to impermeable cells was suggested (20). The most promising CPP is TAT peptide (21), and its fragment TAT_{44-50} sequence as most conservative region could be exploited for pharmaceutical interventions (22). It has been investigated that fragments composed of TAT_{43-60} and TAT_{48-60} sequences possesing safety, and suggested that the shorter peptides could be efficient as well as valuable vectors exploited for drug delivery purpose (23). Among TAT peptide, the cell internalization capability conferred in the Nuclear Localization Signal (NLS) composed of polyarginine bunch in TAT sequence $_{48-57}$ (23,24). It has also shortlisted that romoval of first amino acid in the TAT sequence $_{48-57}$ resulted no significant effect and that it retained the cell penetratibility capacity (25-27). The tranlocation of cell penetrating peptides into cell membrane and delivery of drug molecules into the nucleus considered through endocytosis and direct translocation mechanisms (28).

The physico-chemical properties of drugs such as molecular weight, shape, charge and aqueous solubility as well as its cellular uptake determine the rate of diffusion into the tissue (4). The

presence of high density of basic amino acid residues (Arg and Lys) presents cationic charges that may facilitate the transduction of peptides into the cell (29). The cationic CPPs electro-statically bind with the anionic charges of the plasma membrane lipid contents (30) while the negative charge on the cytoplasmic side of the membrane and the electrostatic interaction may concentrate the peptide on the cell surface and lead to enhancement of internalization (31). In addition to other reasons for the failure of drug or biomarker to penetrate in tumors, one major reasons is the increased interstitial fluid pressure due to leaky vasculature and poor lymphatic drainage in tumor tissue as well as hindered diffusion due to condensed cell packing and extracellular matrix (32). Tumor cells response is different to therapeutic factors *in-vitro* as compared to *in-vivo*, due to lack of complex interactions within their specialized microenvironments. There is found significant distinctions in morphology, drug resistance, gene expression, and model matrices between 2-D and 3-D cultures, while 3-D MCTS model more closely mimic the *in-vivo* conditions (33). The penetrability (34) and cytotoxicitiy studies (33) through CLSM conducted for nanoformulation including anticancer drugs, and therefore an established penetration measurement technique/protocol could be of greater interest in the field of biomedical research.

Therefore, penetration into the spheroid represents a balance between diffusion in the extracellular space *versus* binding to cell surface that facilitates internalization into the cell. Age of spheroids can be co-related to the age of *in-vivo* tumor and its characteristic features, such as, hypoxia and necrosis. It was hypothesised that individual spherid geometry will play a vital role in TAT-labelled peptide penetraton. Moreover, oldage spheroids could signicantly contribute resistance to penetration of TAT. The objectives of this study was to uncover the spheroids age effect through imaging by confocal microscopy, and hence to investigate whether spheroid age to be corelated with *in-vivo* tumors.

2. Materials and Methods

2.1 Monolayer cell culture

HT-29 cell line was kindly provided by a colleague in the drug delivery group, stocked in Manchester Pharmacy School, The University of Manchester (UK). HT-29 cell line seeded in T-75 cm^2 flasks (Corning® Ltd, St Davids Park, UK) at the rate of 10^4 cells/cm^2 in cell culture media composed of DMEM containing 4.5 g/L glucose (Invitrogen, Paisley, UK) supplemented with 10% foetal bovine serum (FBS) purchased from (Invitrogen, Paisley, UK) and 1% (v/v) each of penicillin/streptomycin (P/S) purchased from (Sigma,Welwyn Garden City, UK) and L-glutamine (Invitrogen, Paisley, UK). Flasks were kept in incubator maintained at 37°C, humidified atmosphere and 5% CO2. Media was changed on alternate day. When cell confluence reached up to 80%, the media was removed, and cells were washed with phosphate buffer saline (PBS) solution (Sigma, Welwyn Garden City, UK). Afterwards, cells were trypsinized by 1% trypsin/EDTA (Sigma, Welwyn Garden City, UK) and kept in incubator at 37°C for further 5 min to detach cells from the flask surface. After detachment, 3 mL of media was added to the cell suspension to neutralize the trypsinization. Cell suspension was pipetted out several times in the flask to disaggregate the cell clumps and transferred to a 15 mL centrifuge tube (Corning® Ltd, St Davids Park, UK) for centrifugation at 112 g for 5 min. The supernatant was decanted, and pellets were re-suspended in PBS solution. Cell number per mililitre of this cell susoension were counted through haemocytometer using light microscope (Olympus UK & Ireland, Southend-on-Sea, UK), and a volume containing specified number of cells were re-seeded/used for MCTS generation.

2.2 Multicellular tumor spheroids generation

Spheroids were generated by liquid overlay technique (35). A 200 µL cell suspension consist of 2000 cells/well were transferred through pipette to each well of 96-well plate (Corning® Ltd, St Davids Park, UK). The 96-well plates were already coated with agarose gel (1.5% w/v), i.e agarose powder (Sigma, Welwyn Garden City, UK) 1.5g dissolved in 100 mL Dulbecco's Modified Eagle's Medium (DMEM) without phenol red (Invitrogen, Paisley, UK). The cell suspension composed of

cell culture media, DMEM with phenol red (Invitrogen, Paisley, UK) containing 4.5 g/litre glucose supplemented with 10% FBS, 1% (v/v) each of P/S and L-glutamine. The seeded 96-well plates were kept in incubator maintained at 37°C, humidified atmosphere and 5% CO_2 for three days without any interruption for complete spheroid generation.

2.3 Criteria for spheroids selection

After three days, all wells of 96-well plates were checked through light microscope for the formation and the shape of spheroids. Only those spheroids were selected for experimental observations which were of spherical shape and the same size after three days of spheroid generation and retained the same characteristics until the day of the observation/ experiment.

2.4 TAT-TAMRA and Spheroids adjustment on microscope

TAT-TAMRA (TATsequence $_{47\text{-}57}$; TAMRA-YGRKKRRQRRR) purchased from (Anaspec Inc, UK). A 0.1 mM Stock solution was prepared in distilled water and then 5 µM working solution was prepared from the stock solution in PBS. A 35 mm petridish (Corning, USA) was fixed in temperature controller on the stage of the confocal microscope (LSM510 Meta/confocor II, Zeiss Germany). Temperature controller switched on and adjusted at the desired temperature (37°C or 7°C). When the desired temperature achieved on the temperature controller scale, then 300 µl of TAT-TAMRA solution was added into the centre of the petridish. After a short interval (approximately 2-3 min), the petridish with solution reached the specified temperature and the temperature reading on the temperature controller scale became stable. A spheroid was taken from 96-well plate, washed three times with phosphate buffer saline and transferred into the centre of the TAT-TAMRA solution in the petridish. The spheroids were focused for observation through the confocal microscope with a microscope objective/ numerical aparture 10x/0.3. TAT-TAMRA was excited at 543 nm wavelength using Helium-Neon (He-Ne) laser. Detector gain and laser intensity were adjusted to get quality images. First observation was taken after 5 min from the time of insertion of the spheroid in TAT-TAMRA solution by conducting optical sectioning and then each 10 min intervals until 95 min.

2.5 Tracking confocal images and data analysis

Images of spheroid were taken at intervals of 3 µm depth starting from the surface of spheroids, using He-Ne Laser at a wavelength 543 nm for excitation of the TAMRA fluorophore (TAT-labelled peptide). The images obtained through confocal software (Carl Zeiss, Germany) were exported to Image-J to produce data by defining a region of interest (ROI) at the center of 2-D image and recorded the average intensity for the same ROI in all images of the image-stack. The ROI was circular in shape and area was approximately 5575 μm^2 which remain consistent from the surface of spheroid up to the interior final observation. The MCTS depth profile (the position of fluorophore(s) along the depth of spheroids) and accumulation of TAT with respect to exposure time were elucidated.

The measured intensity of ROI was transferred from Image-J file to Excel file. The line charts of average intensity were drawn as depth profile *versus* fluorescence intensity in Excel file. The start of each line shows the surface of spheroid(s) towards in-depth of spheroids (up to approximately 100 µm) as shown in Figures 2. The intensity at each time-point was averaged (by sum of intensities of slices divided by the number of slices) and a graph was drawn as a relative accumulation *versus* exposure time as shown in Figure 3. To find out the accumulation of TAT peptide with respect to initial values, that data in Figure 3 was divided by their respective first values, which make the first value equal to 1 and the subsequent values increase with respect to 1 (as shown in Figure 4) which explain the pattern of distribution/penetration of TAT peptide in spheroids.

2.6 Statistical analyses

Statistical analyses were conducted while using two way ANOVA or t-test. The *p*-values less than 0.05 were considered as statistically significant.

3. Results

3.1 Distribution of labelled TAT in spheroids under various conditions

The images revealed a non-uniform distribution within the spheroids. Some of it strongly labeled regions indicating substantial cellular uptake. Other dark areas in much lower fluorescent intensity suggest that either TAT has failed to penetrate or the space is mainly occupied by cells that have not taken up TAT, as shown in Figure 1.

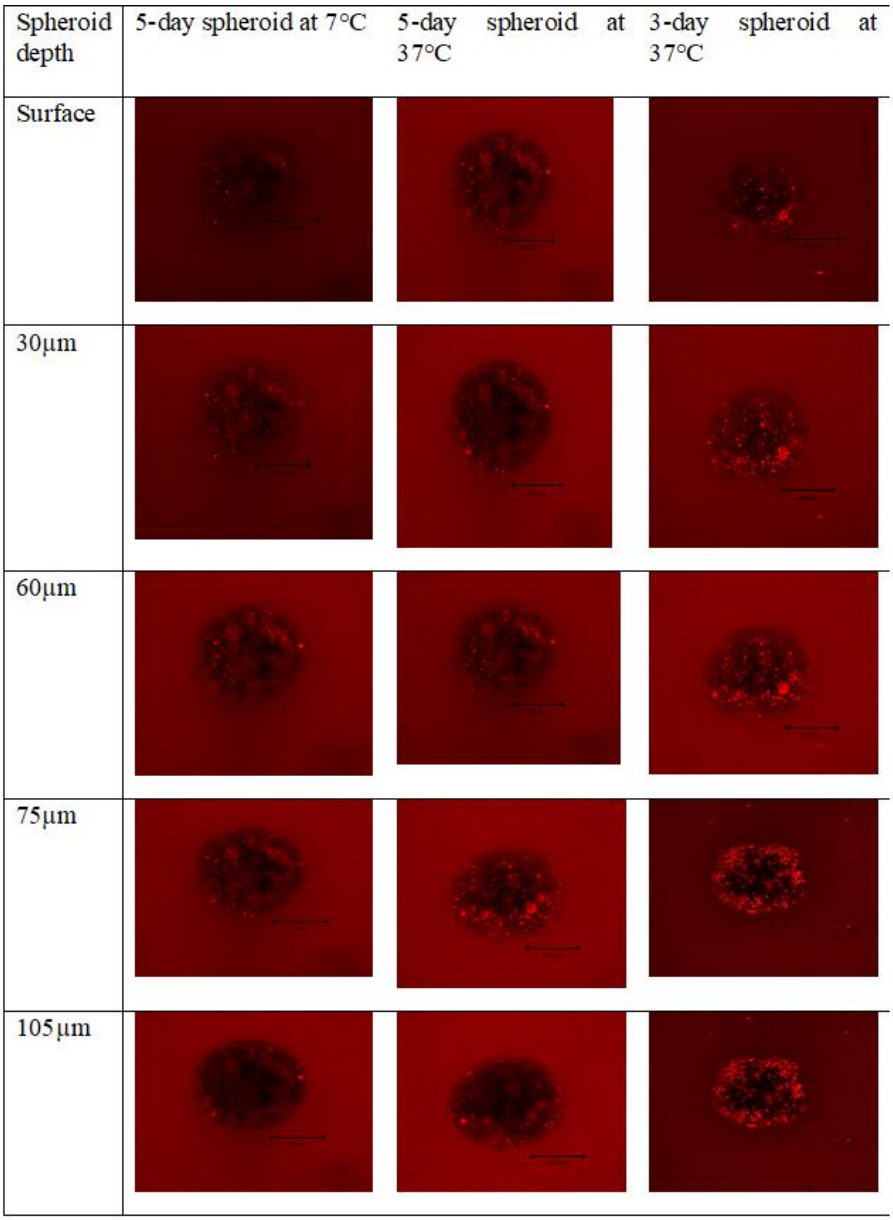

Figure 1. Effect of morphology of spheroid on the penetration of TAT peptide. Confocal image of spheroid at 7 and 37°C depicted here after one-hour exposure in 5 µM TAT solution. It shows the difference in concentration of TAT peptide along the shell of the spheroid, and suggest that spheroid geometry/internal morphology is not exactly divided into distinct layers, rather diversity exists.

In addition to morphology, sequential optical sections of spheroids were collected and analyzed to accumulate fluorescently labeled TAT. Each image data set was processed first to calculate the accumulation of fluorescence as a function of distance into the spheroid along the optical axis

(Figures 2-4). The average fluorescence in the central region of interest was normalized by the intensity of free TAT in the incubating solution. These figures indicate that the average concentration of TAT within the spheroids was always less than the bulk solution (5 µM). However, some sub-regions had much higher local concentrations (at the level of individual cells). The second measure of labeled TAT accumulation was the integrated fluorescence with the same region across all optical sections of the spheroid (from the spheroid surface to a depth of approximately 100 µm). The various aspects of TAT penetration based on the age of spheroids and temperature variation have been presented in Figures 2-4, where, it show that fluorescence intensity (hence penetration) of TATpeptide increases along the exposure time and the effect is statistically significant (ANCOVA, $p < 0.0001$) in all three set of conditions.

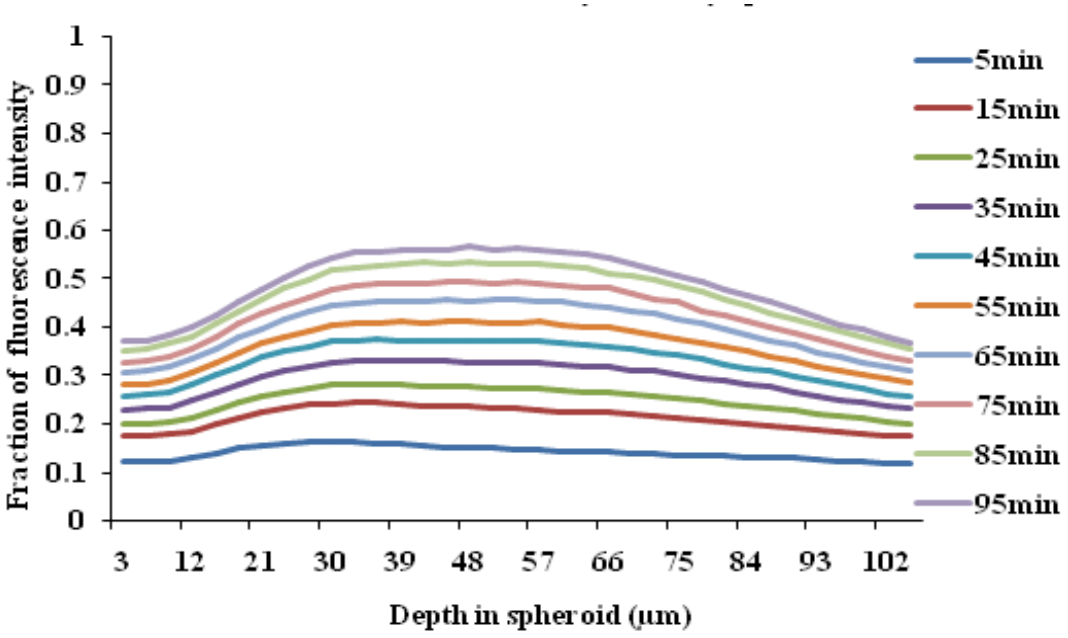

Figure 2. Fluorescence intensity of TAT peptide in 5-day old spheroid at 7ºC

.

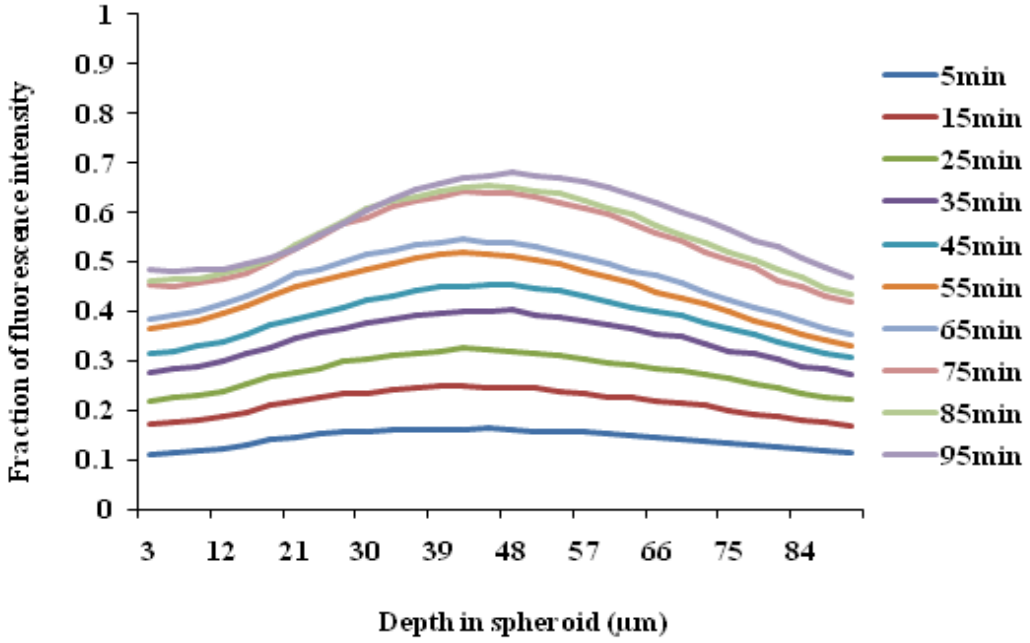

Figure 3. Fluorescence intensity of TAT peptide in 5-day old spheroids at 37ºC.

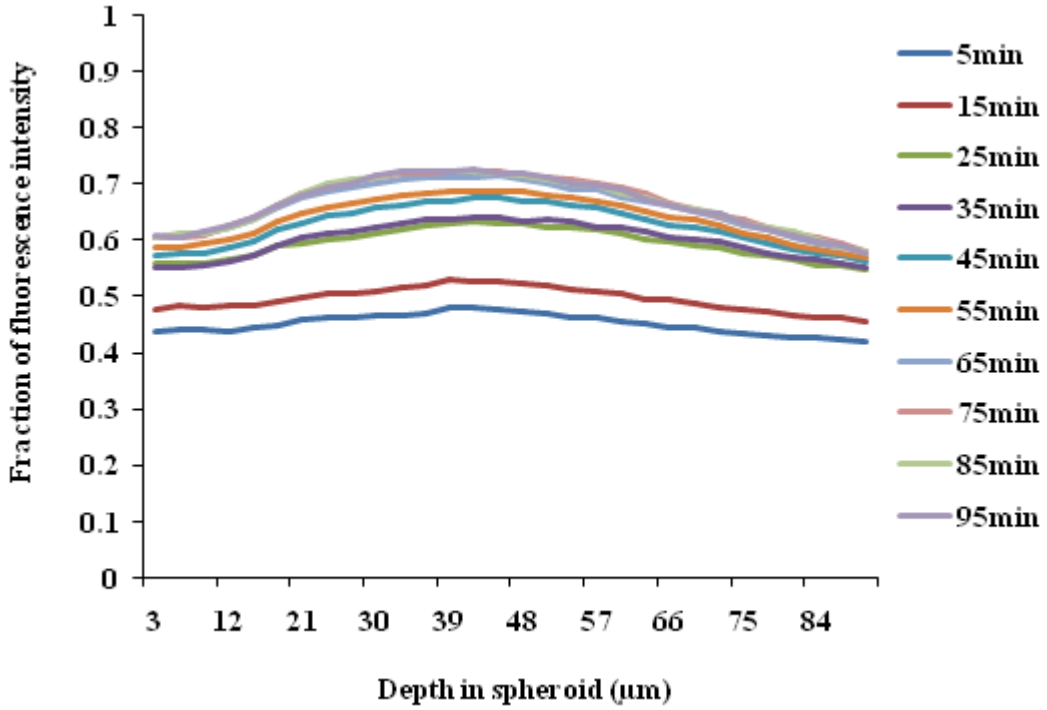

Figure 4. Fluorescence intensity of TAT peptide in 3-day day old spheroid at 37ºC

The graphical representation of fluorescence *versus* depth profile (Figures 2-4) indicates that on the time scale of 90 min, the labeled TAT accumulates at approximately the same rate at each observed depth. The lack of a "moving front" of fluorescence and the location of the highest intensity at some depth (approximately 30-50 µm) into the spheroid suggests that TAT diffusion into the spheroid is relatively rapid and not the limiting factor for accumulation.

3.2 Relative accumulation of TAT in spheroids with respect to exposure time

To compare the relative accumulation of TAT-labelled peptide in spheroids with respect to exposure time, the fluorescence *versus* depth data (Figures 2-4) were averaged over the range of spheroids' depth to generate a measure of accumulation at each time-point. The calculated value represents the accumulation within a spheroid's "core" extending from the surface to a depth of approximately 90 µm, where a value of 1 represents the amount of TAT contained in the same volume of the free solution. Figure 5 demonstrates the relationship between relative accumulation of fluorescence intensity and exposure time for each condition, taking exposure time on X-axis and relative accumulation on Y-axis.

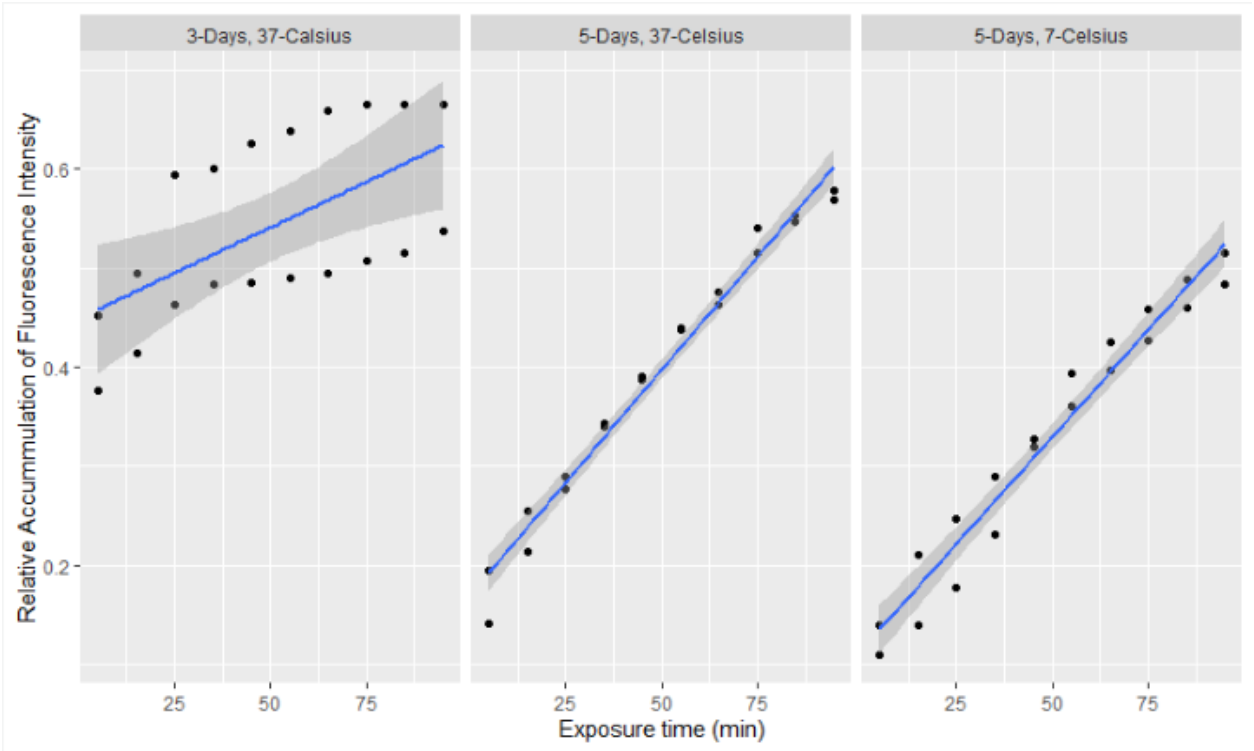

Figure 5. Relative accumulation of TAT peptide in spheroids with respect to exposure time at different conditions. The relative accumulation was calculated by dividing the spheroid fluorescence intensity by their average cell-free solution intensity at each time point. The results suggest earlier saturation in an age-dependent and more accumulation in a temperature-dependent manner.

The graphical representations in Figure 5 show linear relationships for each three conditions with a smaller slope (rate of change) and greater intercept for 3-day old spheroid at 37°C as compared to the other two conditions. The regression analysis results indicate a relatively low rate of change in the fluorescence intensity for 3-days old spheroid at 37°C as compared to the 5-day old spheroid. Further, the Analysis of Covariance (ANCOVA) results show that exposure time has a statistically significant effect on fluorescence intensity after the results adjusted for age and temperature of the spheroids. The results further show that approximately 85% of varibility in the response variable (Relative Accumulation of Fluorescence Intensity) is due to the its association with exposure time and specified conditions as the coefficient of determination (R^2) was calculated as 0.849.

The more accumulation of TAT peptide in 3-day old spheroids is possibly due to the loosely packed cells as compared to 5-day old spheroids. Moreover, 3-day old spheroids have more ratio of proliferating cells as compared to 5-day old spheroids. This high ratio of proliferating cells may have more affinity to TAT uptake; hence accumulation of TAT is greater in 3-day compared to 5-day old spheroids. Moreover, along with the growth of spheroids, the number of proliferating cells decreases [24], resulting in the uptake of peptides will also decrease. The literature shows some controversies, some authors reported that penetration of TATpeptide is temperature dependent [3, 25, 26], while others observed that TAT-peptide penetration is independent of temperature [27-29]. Furthermore, results show that the relative fluorescence accumulation in 3-day old spheroid is higher than 5-day old spheroid, which might be due to early saturation of 3-day old spheroids and a regular increase in accumulation of accumulation fluorescently labeled TAT peptide in 5-day old spheroids. These results are consistent with our hypothesis that spheroids' geometry/distinct cellular distribution changes over time and could alter the penetration of TAT peptides in spheroids.

3.3 Accumulation of TAT in spheroids with respect to initial values

In addition to the penetration depth profile and relative accumulation of Tat-labelled peptide in spheroids, the accumulation concerning initial values is considerably vital that will help in figuring

out the pattern of penetration. The relative accumulation values of each set of conditions were divided by their respective first values. Then curves were plotted by taking exposure time on X-axis and accumulation on the Y-axis, as provided in Figure 6.

The graphs and linear regression analysis results show a strong linear relationship between the Accumulation of TaT (the response variable) and exposure time (independent variable). Further, the ANCOVA results show a significant effect of exposure time and age/temperature of the spheroids.

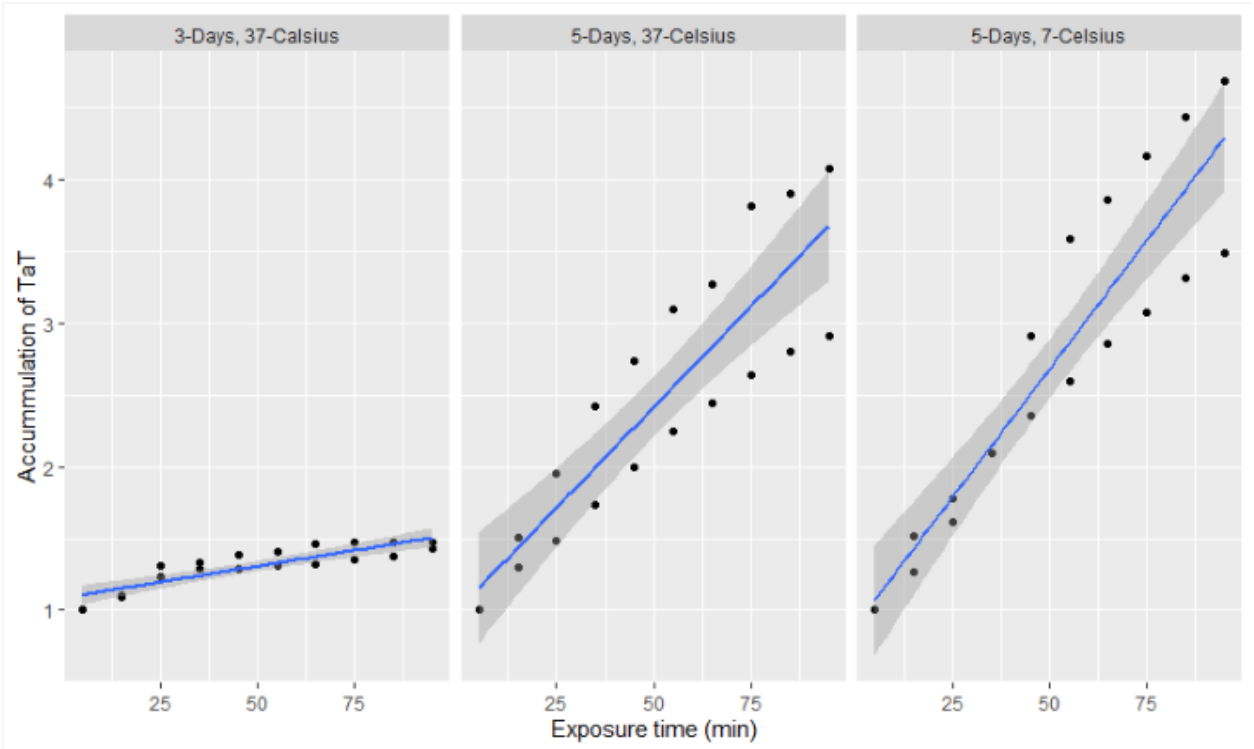

Figure 6. Accumulation of TAT peptide in spheroids at different conditions with respect to initial values. The initial value at each condition was rounded up to one by dividing all values of relative accumulation at each condition with their respective first values.

4. Discussion

Depending on various conditions of spheroids like temperature [3] and age of spheroids [4], the penetration of peptide varies because the larger spheroids develop necrotic and hypoxic regions. The morphology/distinct cellular distribution changes along with age, from spheroid to spheroid or even in the same spheroid, which plays an essential role in TAT peptide penetration. These results confirmed that spheroid's geometry/distinct cellular distribution changes with the passage of time and could alter TAT peptide penetration in spheroids. It was hypothesized that penetration of TAT peptide is temperature-dependent, i.e. the higher the temperature, comparatively more will be the penetration. Here results showed that the penetration of TATpeptide at higher temperature (37°C) was greater than at lower temperature (7°C), and the effect is significant (t, $p < 0.05$). The accumulation in 3-day old spheroid is notable for its higher average intensity, which is particularly evident in the initial phase of the incubation; in the initial scans, the average intensity of 3-day spheroid is more than double the intensity of 5-day spheroid. A likely interpretation of this difference is that the younger spheroid is less compacted and more extracellular volume exist. It is expected that the labeled TAT could rapidly diffuse throughout this extracellular volume, with the extracellular TAT concentration quickly equilibrating with the incubating solution.

Similarly, the average fluorescence intensity at 37°C in 5 days old spheroid is slightly greater as compared to 7°C. It suggests that penetration increases as temperature increases. The effect of TAT

penetration with respect to exposure time is statistically significant, at both temperatures and the age of spheroids (ANCOVA, $p < 0.0001$).

The greater accumulation in 3-day old spheroid compared to 5-day old spheroids justifies one of our hypotheses that TAT penetration may be inversely proportional to the age of spheroids because of the increase in spheroid age, the ratio of proliferating cells decreases and hence penetration of TAT peptide decreases. The accumulation concerning initial values in spheroids was in the order of 5-day old spheroid at 7°C, greater than 5-day old spheroid at 37°C, greater than 3-day old spheroid at 37°C. It suggests that spheroids at 37°C saturate with peptide earlier than spheroids at 7°C, because the relative accumulation of peptide at 37°C is higher than 7°C.

Conclusion

The study was focussed on measuring the uptake of the TAT peptide within spheroids through confocal laser scanning microscopy. It was found that accumulation of TAT-labelled peptide with respect to exposure time and temperature was at the order of 3-day old spheroid at 37°C greater than 5-day old spheroid at 37°C greater than 5-day old spheroid at 7°C. A greater and rapid accumulation of labelled peptide in less developed (3-day) spheroids might be attributed to their greater extracellular volume fraction and more ratio of proliferating cells. The detection of the highest intensity at some depth (approximately 30-50 µm) into the spheroid suggests that TAT diffusion upto this depth is relatively rapid and not the limiting factor for accumulation. However, further low detection, particularly in old spheroid (5-day old) represent either the strong cell-cell contacts as a barrier, inheritent changes inside spheroids or the inherient failure of confocal microscope to measure penetration up to the deeper level. Furthermore, confocal microscopy studies in conjunction with flow cytometry are required to investigate the penetration of TAT in depth along the age of spheroids.

Conflict of Interest: Authors declare no conflict of interest.

Acknowledgements: The principal author is thankful to Dr. David Berk and Dr. Alain Pluen for their contributions in technical assistance and data analysis at Manchester Pharmacy School. This research was financialy supported by Higher Education Commission (HEC) Pakistan through University of Malakand, and Manchester Pharmacy School, The University of Manchester, UK.

References

1. M. Millard, I. Yakavets, V. Zorin, A. Kulmukhamedova, S. Marchal, L. Bezdetnaya, Drug delivery to solid tumors: The predictive value of the multicellular tumor spheroid model for nanomedicine screening, Int J Nanomedicine, 12 (2017) 7993.
2. G. Mehta, A.Y. Hsiao, M. Ingram, G.D. Luker, S. Takayama, Opportunities and challenges for use of tumor spheroids as models to test drug delivery and efficacy, Journal of controlled release : official journal of the Controlled Release Society, 164 (2012) 192-204.
3. I.M. Kaplan, J.S. Wadia, S.F. Dowdy, Cationic TAT peptide transduction domain enters cells by macropinocytosis, yes, 102 (2005) 247-253.
4. A.I. Minchinton, I.F. Tannock, Drug penetration in solid tumours, Nat Rev Cancer, 6 (2006) 583-592.
5. A. Ur Rahman, S. Khan, M. Khan, Transport of trans-activator of transcription (TAT) peptide in tumour tissue model: evaluation of factors affecting the transport of TAT evidenced by flow cytometry, Journal of Pharmacy and Pharmacology.
6. L. Patel, J. Zaro, W.-C. Shen, Cell Penetrating Peptides: Intracellular Pathways and Pharmaceutical Perspectives, Pharmaceutical Research, 24 (2007) 1977-1992.
7. D. Mann, A. Frankel, Endocytosis and targeting of exogenous HIV-1 TAT protein, The EMBO journal, 10 (1991) 1733-1739.

8. M. Hällbrink, A. Florén, A. Elmquist, M. Pooga, T. Bartfai, Ü. Langel, Cargo delivery kinetics of cell-penetrating peptides, Biochimica et Biophysica Acta (BBA) - Biomembranes, 1515 (2001) 101-109.
9. J.C. Mai, H. Shen, S.C. Watkins, T. Cheng, P.D. Robbins, Efficiency of Protein Transduction Is Cell Type-dependent and Is Enhanced by Dextran Sulfate, J. Biol. Chem., 277 (2002) 30208-30218.
10. G. Tunnemann, R.M. Martin, S. Haupt, C. Patsch, F. Edenhofer, M.C. Cardoso, Cargo-dependent mode of uptake and bioavailability of TAT-containing proteins and peptides in living cells, FASEB J., 20 (2006) 1775-1784.
11. S.D. Conner, S.L. Schmid, Regulated portals of entry into the cell, Nature, 422 (2003) 37-44.
12. P. Watson, A.T. Jones, D.J. Stephens, Intracellular trafficking pathways and drug delivery: fluorescence imaging of living and fixed cells, Advanced Drug Delivery Reviews, 57 (2005) 43-61.
13. P. Järver, Ü. Langel, Cell-penetrating peptides--A brief introduction, Biochimica et Biophysica Acta (BBA) - Biomembranes, 1758 (2006) 260-263.
14. A. Chauhan, A. Tikoo, A.K. Kapur, M. Singh, The taming of the cell penetrating domain of the HIV TAT: Myths and realities, yes, 117 (2007) 148-162.
15. J. Liu, F. Yan, H. Chen, W. Wang, W. Liu, K. Hao, G. Wang, F. Zhou, J. Zhang, A novel individual-cell-based mathematical model based on multicellular tumour spheroids for evaluating doxorubicin-related delivery in avascular regions, British journal of pharmacology, 174 (2017) 2862-2879.
16. B. Gupta, T.S. Levchenko, V.P. Torchilin, Intracellular delivery of large molecules and small particles by cell-penetrating proteins and peptides, Advanced Drug Delivery Reviews, 57 (2005) 637-651.
17. J. Howl, I.D. Nicholl, S. Jones, The many futures for cell-penetrating peptides: how soon is now?, Biochemical Society Transactions, 035 (2007) 767-769.
18. M. Green, P.M. Loewenstein, Autonomous functional domains of chemically synthesized human immunodeficiency virus TAT trans-activator protein, Cell, 55 (1988) 1179-1188.
19. A.D. Frankel, C.O. Pabo, Cellular uptake of the TAT protein from human immunodeficiency virus, Cell, 55 (1988) 1189-1193.
20. S. Fawell, J. Seery, Y. Daikh, C. Moore, L.L. Chen, B. Pepinsky, J. Barsoum, TAT-mediated delivery of heterologous proteins into cells, Proceedings of the National Academy of Sciences of the United STATes of America, 91 (1994) 664-668.
21. M. Popovic, M.G. Sarngadharan, E. Read, R.C. Gallo, Detection, isolation, and continuous production of cytopathic retroviruses (HTLV-III) from patients with AIDS and pre-AIDS, Science, 224 (1984) 497-500.
22. S. Pantano, P. Carloni, Comparative analysis of HIV-1 TAT variants, Proteins: Structure, Function, and Bioinformatics, 58 (2005) 638-643.
23. E. Vives, P. Brodin, B. Lebleu, A Truncated HIV-1 TAT Protein Basic Domain Rapidly Translocates through the Plasma Membrane and Accumulates in the Cell Nucleus, J. Biol. Chem., 272 (1997) 16010-16017.
24. B. Cornelissen, M. Hu, K. McLarty, D. Costantini, R.M. Reilly, Cellular penetration and nuclear imporTATion properties of 111In-labeled and 123I-labeled HIV-1 TAT peptide immunoconjugates in BT-474 human breast cancer cells, Nuclear Medicine and Biology, 37 (2007) 37-46.
25. S. Futaki, T. Suzuki, W. Ohashi, T. Yagami, S. Tanaka, K. Ueda, Y. Sugiura, Arginine-rich Peptides. AN ABUNDANT SOURCE OF MEMBRANE-PERMEABLE PEPTIDES HAVING POTENTIAL AS CARRIERS FOR INTRACELLULAR PROTEIN DELIVERY, J. Biol. Chem., 276 (2001) 5836-5840.
26. V. Polyakov, V. Sharma, J.L. Dahlheimer, C.M. Pica, G.D. Luker, D. Piwnica-Worms, Novel TAT-Peptide Chelates for Direct Transduction of Technetium-99m and Rhenium into Human Cells for Imaging and Radiotherapy, Bioconjugate Chem., 11 (2000) 762-771.

27. P.A. Wender, D.J. Mitchell, K. Pattabiraman, E.T. Pelkey, L. Steinman, J.B. Rothbard, The design, synthesis, and evaluation of molecules that enable or enhance cellular uptake: Peptoid molecular transporters, Proceedings of the National Academy of Sciences of the United STATes of America, 97 (2000) 13003-13008.
28. M. Kristensen, D. Birch, H. Mørck Nielsen, Applications and Challenges for Use of Cell-Penetrating Peptides as Delivery Vectors for Peptide and Protein Cargos, International Journal of Molecular Sciences, 17 (2016) 185.
29. A. Ho, S.R. Schwarze, S.J. Mermelstein, G. Waksman, S.F. Dowdy, Synthetic Protein Transduction Domains: Enhanced Transduction Potential in Vitro and in Vivo, Cancer research, 61 (2001) 474-477.
30. A. Ziegler, Thermodynamic studies and binding mechanisms of cell-penetrating peptides with lipids and glycosaminoglycans, Advanced Drug Delivery Reviews, 60 (2008) 580-597.
31. S. Futaki, Oligoarginine vectors for intracellular delivery: Design and cellular-uptake mechanisms, Peptide Science, 84 (2006) 241-249.
32. S. Lu, F. Zhao, Q. Zhang, P. Chen, Therapeutic peptide amphiphile as a drug carrier with ATP-triggered release for synergistic effect, improved therapeutic index, and penetration of 3D cancer cell spheroids, International journal of molecular sciences, 19 (2018) 2773.
33. V.-M. Le, M.-D. Lang, W.-B. Shi, J.-W. Liu, A collagen-based multicellular tumor spheroid model for evaluation of the efficiency of nanoparticle drug delivery, Artificial Cells, Nanomedicine, and Biotechnology, 44 (2016) 540-544.
34. A.M. Privalova, S.V. Uglanova, N.R. Kuznetsova, N.L. Klyachko, Y.I. Golovin, V.V. Korenkov, E.L. Vodovozova, E.A. Markvicheva, Microencapsulated multicellular tumor spheroids as a tool to test novel anticancer nanosized drug delivery systems in vitro, Journal of nanoscience and nanotechnology, 15 (2015) 4806-4814.
35. J. CARLSSON, K. NILSSON, B. WESTERMARK, J. PONTEN, C. SUNDSTROM, E. LARSSON, J. BERGH, S. PAHLMAN, C. BUSCH, V.P. COLLINS, FORMATION AND GROWTH OF MULTICELLULAR SPHEROIDS OF HUMAN ORIGIN, Int. J. Cancer 31 (1983) 523-533.
36. R.M. Sutherland, Cell and environment interactions in tumor microregions: the multicell spheroid model, Science, 240 (1988) 177-184.
37. J.P. Richard, K. Melikov, H. Brooks, P. Prevot, B. Lebleu, L.V. Chernomordik, Cellular Uptake of Unconjugated TAT Peptide Involves Clathrin-dependent Endocytosis and Heparan Sulfate Receptors, J. Biol. Chem., 280 (2005) 15300-15306.
38. M. Lindgren, M. Hällbrink, A. Prochiantz, Ü. Langel, Cell-penetrating peptides, Trends in Pharmacological Sciences, 21 (2000) 99-103.